# A three-dimensional numerical method for thermal analysis in X-ray lithography

W. Dai and R. Nassar

*Mathematics and Statistics, College of Engineering and Science, Louisiana Tech University, Ruston, USA*

Received February 1997
Revised June 1997
Accepted September 1997

## 1. Introduction

X-ray irradiation of photoresists, such as polymethylmethacrylate (PMMA), on a silicon substrate is an important technique in micro fabrication used to obtain structures and devices with a high aspect ratio. The process is composed of a mask and a photoresist deposited on a substrate (with a gap between mask and resist). The mask layer creates a desired pattern on the photoresist by selectively allowing the transmission of irradiation from an X-ray beam. After exposure, the photoresist is developed to remove the irradiated area, leaving behind an imprint of the pattern in the form of exposed substrate and photoresist walls. The pattern can now be used as a micromold. Electroplating can then be used to fill the mold with a metal. The remaining unexposed part of the photoresist can then be removed by an etchant, leaving the free standing microstructure on the substrate.

Predictions of the temperature distribution in three dimensions in the different layers (mask, gap, photoresist and substrate) and of the potential temperature rise in the resist are essential for determining the effect of high flux X-ray exposure on distortions in the photoresist due to thermal expansion. A thorough understanding of the problem has been hampered by the difficulties involved in finding solutions to elliptic or parabolic differential equations describing temperature profiles in multilayers. Analytic solutions to the system of these differential equations describing the process are not easy to obtain due to the complication of the three-dimensional case and the fact that the value at the interfacial boundary between layers is unknown. Only a few studies have considered these kind of problems in the literature (Ameel *et al.*, 1994; Cole and McGahan, 1993; Kant, 1988; Madison and McDaniel, 1989). Recently, Dai *et al.* (1997) have developed numerical heat transfer models for thermal analysis in X-ray irradiated photoresists. The steady state temperature distribution in the resist has been obtained by solving the unsteady state differential equations in the case of two layers, resist and substrate. In this article, we develop a numerical method to

This research is supported by a Louisiana Educational Quality Support Fund grant, Contract No: 72-6000792.

International Journal of Numerical Methods for Heat & Fluid Flow
Vol. 8 No. 4, 1998, pp. 409–423.

investigate the temperature distribution in a commercially applicable X-ray irradiation process, where the target consists of a mask, a resist and a substrate (with a gap between mask and resist). In this method, the preconditioned Richardson method will be applied for solving the Poisson equation in the micro-scale to obtain the steady state temperature. A domain decomposition algorithm will then be obtained based on the parallel "divide and conquer" procedure, which overcomes the problem with the unknown value at the interface. Such a method is simple and fast, which is compared with the previous methods.

## 2. X-ray irradiation process

We now consider a commercially applicable X-ray irradiation process, where the target consists of a mask, a resist and a substrate (with a gap between mask and resist), as shown in Figure 1 (mask, resist and substrate are held in place through a special clamping mechanism not shown in the figure). A gap exists between mask and resist through which air circulates to prevent overheating on the exposed area of the resist. The resist such as PMMA is placed on a substrate, such as silicon. The mask, resist and substrate are very thin, of the order of 300μm, with a square dimension of 5mm × 5mm, for instance. The gap is also very thin, of the order of 50 μm, for instance. To study the effect of the high flux X-ray exposure on distortions in the resist, it is important to predict the temperature distribution in the resist and the substrate. Heat from the X-ray beam is first transferred by conduction through the mask. Owing to the very thin gap and the relatively low temperature, radiation can be neglected. Also, convection in the gap is small relative to conduction . Hence, without loss of generality, we assume that heat is mainly transferred by conduction through the gap. Heat is then transferred

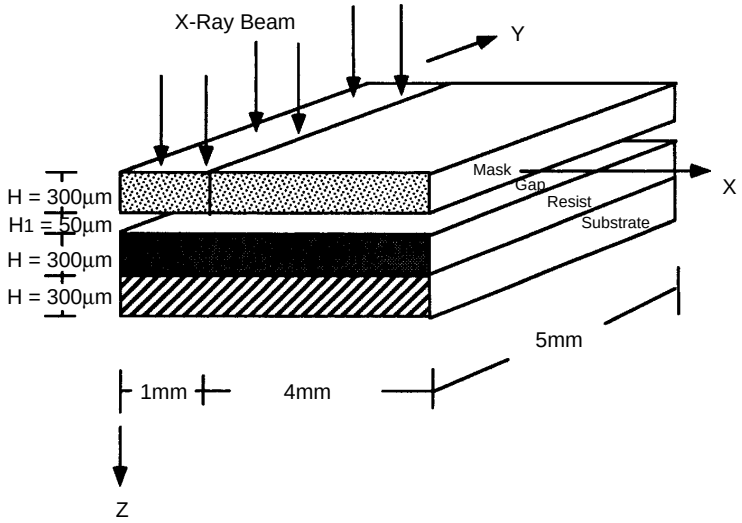


**Figure 1.**
Configuration of an X-ray irradiated process

by conduction through the resist and substrate. As such, the governing equations for temperatures at steady state in the mask, gap, resist and substrate are given by the elliptic equations (Ameel *et al.*, 1994; Incropera and Dewitt, 1985; Ozisik, 1980):

Mask

$$-k_1\left(\frac{\partial^2 T_1}{\partial x^2}+\frac{\partial^2 T_1}{\partial y^2}+\frac{\partial^2 T_1}{\partial z^2}\right)=g(x,y,z); \tag{1}$$

Gap

$$-k_2\left(\frac{\partial^2 T_2}{\partial x^2}+\frac{\partial^2 T_2}{\partial y^2}+\frac{\partial^2 T_2}{\partial z^2}\right)=g(x,y,z); \tag{2}$$

Resist

$$-k_3\left(\frac{\partial^2 T_3}{\partial x^2}+\frac{\partial^2 T_3}{\partial y^2}+\frac{\partial^2 T_3}{\partial z^2}\right)=g(x,y,z); \tag{3}$$

Substrate

$$-k_4\left(\frac{\partial^2 T_4}{\partial x^2}+\frac{\partial^2 T_4}{\partial y^2}+\frac{\partial^2 T_4}{\partial z^2}\right)=g(x,y,z); \tag{4}$$

where $T_1$, $T_2$, $T_3$, $T_4$, $K_1$, $K_2$, $K_3$, $K_4$ are temperatures, and conductivities, respectively. The source term $g(x, y, z)$ depends on the mode of operation of the system and can be determined by experiments. The boundary conditions are described as follows.

On the top surface of the mask, $z = 0$, where heat convection occurs,

$$k_1\frac{\partial T_1}{\partial z}=h_c(T_1-T_\infty), \tag{5}$$

where $T_\infty$ is the temperature of the surroundings and $h_c$ is the convection coefficient.

On the bottom surface of the mask, $z = H$, we assume that the flux across the interface does not change,

$$-k_1\frac{\partial T_1}{\partial z}=-k_2\frac{\partial T_2}{\partial z}, \quad \text{and} \quad T_1=T_2. \tag{6}$$

Similarly, on the top surface of the resist, $z = H + H_1$,

$$-k_2\frac{\partial T_2}{\partial z}=-k_3\frac{\partial T_3}{\partial z}, \quad \text{and} \quad T_3=T_2. \tag{7}$$

On the bottom surface of the resist, $z = 2H + H_1$,

$$-k_3\frac{\partial T_3}{\partial z} = -k_4\frac{\partial T_4}{\partial z}, \quad \text{and} \quad -k_3\frac{\partial T_3}{\partial z} = h(T_3 - T_4). \tag{8}$$

A finite value $h$ implies the discontinuity of the temperature at the interfaces. When h $\rightarrow\infty$, the second boundary condition in Equation (8) reduces to $T_3 = T_4$, which implies continuity of the temperature or perfect thermal contact at the interface.

Under experimental conditions the side walls of mask, resist and substrate (Figure 1), and the bottom surface of the substrate are kept at a constant temperature or open to the surrounding so as to prevent heat from building-up. As such, it is realistic to assume $T_i = T_\infty$, $i = 1, 2, 3, 4$, at the side walls, and $T_4 = T_\infty$ at the bottom surface of the substrate.

### 3. Preconditioned Richardson iteration

Consider the three-dimensional Poisson equation

$$-\left(\frac{\partial^2 T}{\partial x^2} + \frac{\partial^2 T}{\partial y^2} + \frac{\partial^2 T}{\partial z^2}\right) = f(x, y, z, t) \tag{9}$$

We let $T_{ijk}$ denote the approximation to $T$ ($i\Delta x$, $j\Delta y$, $k\Delta z$), where $\Delta x$, $\Delta y$ and $\Delta z$ are the grid sizes in the $x$, $y$ and $z$ directions, respectively, $i = 0, \ldots, N_x$, $j = 0, \ldots, N_y$ and $k = 0, \ldots, N_z$. We use the centered-difference equation,

$$\frac{1}{\Delta x^2}\delta_x^2 T_{ijk} = \frac{1}{\Delta x^2}\left(T_{i+1jk} - 2T_{ijk} + T_{i-1jk}\right), \tag{10}$$

to approximate

$$\frac{\partial^2 T(x, y, z)}{\partial x^2},$$

and so on. The finite difference scheme for Equation (9) can be expressed

$$-\left(\frac{1}{\Delta x^2}\delta_x^2 + \frac{1}{\Delta y^2}\delta_y^2 + \frac{1}{\Delta z^2}\delta_z^2\right)T_{ijk} = f_{ijk}. \tag{11}$$

Let $\left(A_x\bar{T}\right)_{ijk} = -\frac{1}{\Delta x^2}\delta_x^2 T_{ijk}$, $\left(A_y\bar{T}\right)_{ijk} = -\frac{1}{\Delta y^2}\delta_y^2 T_{ijk}$, and $\left(A_z\bar{T}\right)_{ijk} = -\frac{1}{\Delta z^2}\delta_z^2 T_{ijk}$,

where $A_x$, $A_y$ and $A_z$ are matrices and $\bar{T}$ is a vector consisting of $T_{ijk}$, $i = 1, \ldots, N_x - 1$, $j = 1, \ldots, N_y - 1$ and $k = 1, \ldots, N_z - 1$. Then the system (11) can be written in a vector form:

$$(A_x + A_y + A_z)\bar{T} = \bar{f}. \tag{12}$$

It can be seen (Li and Hong, 1979) that the eigenvalues of $A_z$ are $\frac{4}{\Delta z^2}\sin^2\frac{k\pi\Delta z}{2}$, $k = 1, \ldots, N_z - 1$. Since $\Delta z$ is very small in the micro case, the ratio $\frac{\lambda_{\max}(A_z)}{\lambda_{\min}(A_z)} = 0\left(\frac{1}{\Delta z^2}\right)$ is very large, where $\lambda_{max}(A_z)$ and $\lambda_{min}(A_z)$ are maximum and minimum eigenvalues, respectively. This results in the system (12) being ill-conditioned. Hence, common iteration methods, such as the Gauss-Seidel method, will converge very slowly. To overcome this difficulty, we apply a preconditioning technique and the Richardson iteration on Equation (12). This gives

$$L_{pre}\,\bar{T}^{(n+1)} = L_{pre}\,\bar{T}^{(n)} - \alpha\left[(A_x + A_y + A_z)\bar{T}^{(n)} - \bar{f}\right], \tag{13}$$

where the preconditioner is chosen as follows:

$$L_{pre} \equiv A_z + \left(\frac{4}{\Delta x^2} + \frac{4}{\Delta y^2}\right)I, \tag{14}$$

and $\alpha$ is a relaxation parameter. It is well known from numerical linear algebra that the iteration process converges if the iteration operator

$$B = I - \alpha\, L_{pre}^{-1}(A_x + A_y + A_z) \tag{15}$$

has a spectral radius $\rho(B) < 1$. Further, the smaller $\rho(B)$ is, the faster the iteration converges. It can be shown that the eigenvalue of $L_{pre}^{-1}(A_x + A_y + A_z)$ has the form

$$\lambda_{ijk} = \frac{\frac{4}{\Delta x^2}\sin^2\frac{i\pi\Delta x}{2} + \frac{4}{\Delta y^2}\sin^2\frac{j\pi\Delta y}{2} + \frac{4}{\Delta z^2}\sin^2\frac{k\pi\Delta z}{2}}{\frac{4}{\Delta x^2} + \frac{4}{\Delta y^2} + \frac{4}{\Delta z^2}\sin^2\frac{k\pi\Delta z}{2}}. \tag{16}$$

When $\Delta z$ is very small compared to $\Delta x$ and $\Delta y$, $\lambda_{ijk}$ is dominated by $\frac{4}{\Delta z^2}\sin^2\frac{k\pi\Delta z}{2}$. Hence, $\lambda_{ijk}$ is close to 1. If one chooses a relaxation parameter $\alpha$ which is close to 1, then the spectral radius $\rho(B)$ will be much smaller than 1. Hence, we conclude that the iteration method (13) converges very fast.

We now apply the iteration method (13) to Equations (1)-(4) and write the iteration scheme as follows:

$$\left(-\frac{1}{\Delta z^2}\delta_z^2+\frac{4}{\Delta x^2}+\frac{4}{\Delta y^2}\right)(T_m)_{ijk}^{(n+1)}=\left(-\frac{1}{\Delta z^2}\delta_z^2+\frac{4}{\Delta x^2}+\frac{4}{\Delta y^2}\right)(T_m)_{ijk}^{(n)}$$

$$+\alpha\left(\frac{1}{\Delta z^2}\delta_z^2+\frac{1}{\Delta x^2}\delta_x^2+\frac{1}{\Delta y^2}\delta_y^2\right)(T_m)_{ijk}^{(n)}+\alpha(f_m)_{ijk}, \tag{17}$$

where $m = 1, 2, 3, 4$. At each iteration step, $(T_m)_{ijk}^{(n+1)}$ is assumed to satisfy the discrete boundary conditions. Obviously, for each iteration step four tridiagonal linear systems must be solved simultaneously. We will develop a domain decomposition algorithm, which is based on a parallel "divide and conquer" procedure obtained in the following section, to solve the above four tridiagonal linear systems simultaneously.

## 4. Parallel divide and conquer procedure

As is known, the usual approach for solving the above tridiagonal linear system

$$\begin{cases} -b_i x_{i-1}+a_i x_i-c_i x_{i+1}=d_i, \quad i=1,\cdots,n, \\ x_o=x_{n+1}=0 \end{cases} \tag{18}$$

is the Gaussian elimination technique. This approach results in a procedure called the "divide and conquer" procedure, shown as follows:

$$\beta_k=\frac{c_k}{a_k-b_k\beta_{k-1}}, \quad \beta_o=0, \tag{19a}$$

$$\nu_k=\frac{d_k+b_k\nu_{k-1}}{a_k-b_k\beta_{k-1}}, \quad \nu_o=0; \quad k=1,\cdots,n, \tag{19b}$$

$$x_k=\beta_k x_{k+1}+\nu_k, \quad x_{n+1}=0; \quad k=n,\cdots,1. \tag{19c}$$

In the above procedure, $\beta_k$, $\nu_k$ are calculated from $k = 1$ to $k = n$, while $x_k$ is computed from $k = n$ to $k = 1$. A similar procedure that is opposite in direction can be expressed as

$$\tilde{\beta}_k=\frac{b_k}{a_k-c_k\tilde{\beta}_{k+1}}, \quad \tilde{\beta}_{n+1}=0, \tag{20a}$$

$$\tilde{\nu}_k=\frac{d_k+c_k\tilde{\nu}_{k+1}}{a_k-c_k\tilde{\beta}_{k+1}}, \quad \tilde{\nu}_{k+1}=0; \quad k=n,\cdots,1, \tag{20b}$$

$$x_k=\tilde{\beta}_k x_{k-1}+\tilde{\nu}_k, \quad x_o=0; \quad k=1,\cdots,n. \tag{20c}$$

Further, if $x_0$ and $x_{n+1}$ are not zero, one has

$$\beta_k = \frac{c_k}{a_k - \beta_{k-1} b_k}, \quad \beta_o = 0, \tag{21a}$$

$$\nu_k = \frac{d_k + b_k \nu_{k-1}}{a_k - b_k \beta_{k-1}}, \quad \nu_o = 0, \tag{21b}$$

$$\lambda_k = \frac{b_k \lambda_{k-1}}{a_k - \beta_{k-1} b_k}, \quad \lambda_o = 1; \quad k = 1, \cdots, n, \tag{21c}$$

$$x_k = \beta_k x_{k+1} + \nu_k + \lambda_k x_o; \quad k = n, \cdots, 1, \tag{21d}$$

and

$$\tilde{\beta}_k = \frac{b_k}{a_k - \tilde{\beta}_{k+1} c_k}, \quad \tilde{\beta}_{n+1} = 0, \tag{22a}$$

$$\tilde{\nu}_k = \frac{d_k + c_k \tilde{\nu}_{k+1}}{a_k - c_k \tilde{\beta}_{k+1}}, \quad \tilde{\nu}_{n+1} = 0, \tag{22b}$$

$$\tilde{\lambda}_k = \frac{c_k \tilde{\lambda}_{k+1}}{a_k - \tilde{\beta}_{k+1} c_k}, \quad \tilde{\lambda}_{n+1} = 1; \quad k = n, \cdots, 1, \tag{22c}$$

$$x_k = \tilde{\beta}_k x_{k-1} + \tilde{\nu}_k + \tilde{\lambda}_k x_{n+1}; \quad k = 1, \cdots, n. \tag{22d}$$

Let $n = 4N + 3$ for convenience, we divide the system (18) into four subsystems, which consist of the first $N$ equations, the second $N$ equations, the third $N$ equations and the last $N$ equations. The $(N + 1)th$, the $(2N + 2)th$ and the $(3N + 3)th$ equations designate the interfacial equations. If the above four procedures are combined together, then the parallel "divide and conquer" procedure based on the domain decomposition method (Dai and Nassar, 1997; Ottega, 1988) can be written as follows:

Step 1. Calculate $\left\{ \begin{array}{l} \beta_k^{(1)}, \nu_k^{(1)}, \ k = 1, \cdots, N, \text{ for the first } N \text{ equations by (19ab)} \\ \beta_k^{(2)}, \nu_k^{(2)}, \lambda_k^{(2)}, \ k = 1, \cdots, N, \text{ for the second } N \text{ equations by (21abc)} \\ \tilde{\beta}_k^{(2)}, \tilde{\nu}_k^{(2)}, \tilde{\lambda}_k^{(2)}, \ k = N, \cdots, 1, \text{ for the second } N \text{ equations by (22abc)} \\ \beta_k^{(3)}, \nu_k^{(3)}, \lambda_k^{(3)}, \ k = 1, \cdots, N, \text{ for the third } N \text{ equations by (21abc)} \\ \tilde{\beta}_k^{(3)}, \tilde{\nu}_k^{(3)}, \tilde{\lambda}_k^{(3)}, \ k = N, \cdots, 1, \text{ for the third } N \text{ equations by (22abc)} \\ \tilde{\beta}_k^{(4)}, \tilde{\nu}_k^{(4)}, \ k = N, \cdots, 1, \text{ for the last } N \text{ equations by (20ab)} \end{array} \right\}$ in parallel.

Step 2. Substitute $x_N = \beta_N^{(1)} x_{N+1} + \nu_N^{(1)}$, $x_{2N+1} = \beta_N^{(2)} x_{2N+2} + \nu_N^{(2)} + \lambda_N^{(2)} x_{N+1}$, $x_{N+2} = \tilde{\beta}_1^{(2)} x_{N+1} + \tilde{\nu}_1^{(2)} + \tilde{\lambda}_1^{(2)} x_{2N+2}$, $x_{3N+2} = \beta_N^{(3)} x_{3N+3} + \nu_N^{(3)} + \lambda_N^{(3)} x_{2N+2}$, $x_{2N+3} = \tilde{\beta}_1^{(3)} x_{2N+2} + \tilde{\nu}_1^{(3)} + \tilde{\lambda}_1^{(3)} x_{3N+3}$ and $x_{3N+4} = \tilde{\beta}_1^{(4)} x_{3N+3} + \tilde{\nu}_1^{(4)}$ into $\begin{Bmatrix} -b_{N+1} x_N + a_{N+1} x_{N+1} - c_{N+1} x_{N+2} = d_{N+1} \\ -b_{2N+2} x_{2N+1} + a_{2N+2} x_{2N+2} - c_{2N+2} x_{2N+3} = d_{2N+2} \\ -b_{3N+3} x_{3N+2} + a_{3N+3} x_{3N+3} - c_{3N+3} x_{3N+4} = d_{3N+3} \end{Bmatrix}$, then solve $x_{N+1}$, $x_{2N+2}$ and $x_{3N+3}$.

Step 3. Solve $\begin{Bmatrix} x_k = \beta_k^{(1)} x_{k+1} + \nu_k^{(1)}, \quad k = N, \cdots, 1 \\ x_{N+k+1} = \beta_k^{(2)} x_{N+k+2} + \nu_k^{(2)} + \lambda_k^{(2)} x_{N+1}, \quad k = N, \cdots, 1 \\ x_{2N+k+2} = \beta_k^{(3)} x_{2N+k+3} + \nu_k^{(3)} + \lambda_k^{(3)} x_{2N+2}, \quad k = N, \cdots, 1 \\ x_{3N+k+3} = \tilde{\beta}_k^{(4)} x_{3N+k+2} + \tilde{\nu}_k^{(4)}, \quad k = 1, \cdots, N \end{Bmatrix}$ in parallel.

## 5. Domain decomposition algorithm

To develop a numerical method for predicting the temperature profile, we assume that there is a mesh grid of $N_x \times N_y \times N_z$ for the mask, gap, resist and substrate layers with the same grid size $\Delta x$ and $\Delta y$, where $(N_x + 1)\Delta x = L$, $(N_y + 1)\Delta y = L$. Let $\Delta z$ be a grid size for the mask, resist and substrate such that $(N_z + 1)\Delta z = H$, while $\Delta \tilde{z}$ is a grid size for the gap such that $(N_z + 1)\Delta \tilde{z} = H_1$. The iteration scheme is equation (17) with discrete boundary conditions as follows:

$$k_1 \frac{(T_1)_{ij1}^{(n+1)} - (T_1)_{ij0}^{(n+1)}}{\Delta z} = h_{c1}\left((T_1)_{ij0}^{(n+1)} - T_\infty\right), \quad z = 0, \tag{23a}$$

$$\begin{cases} -k_1 \dfrac{(T_1)_{ijNz+1}^{(n+1)} - (T_1)_{ijNz}^{(n+1)}}{\Delta z} = -k_2 \dfrac{(T_2)_{ij1}^{(n+1)} - (T_2)_{ij0}^{(n+1)}}{\Delta \tilde{z}}, \\ (T_1)_{ijnz+1}^{(n+1)} = (T_2)_{ij0}^{(n+1)}, \end{cases} \quad z = H, \tag{23b}$$

$$\begin{cases} -k_2 \dfrac{(T_2)_{ijNz+1}^{(n+1)} - (T_2)_{ijNz}^{(n+1)}}{\Delta \tilde{z}} = -k_3 \dfrac{(T_3)_{ij1}^{(n+1)} - (T_3)_{ij0}^{(n+1)}}{\Delta z}, \\ (T_2)_{ijNz+1}^{(n+1)} = (T_3)_{ij0}^{(n+1)}, \end{cases} \quad z = H + H_1, \tag{23c}$$

$$\begin{cases} -k_3 \dfrac{(T_3)_{ijNz+1}^{(n+1)} - (T_3)_{ijNz}^{(n+1)}}{\Delta z} = -k_4 \dfrac{(T_4)_{ij1}^{(n+1)} - (T_4)_{ij0}^{(n+1)}}{\Delta z}, \\ -k_3 \dfrac{(T_3)_{ijNz+1}^{(n+1)} - (T_3)_{ijNz}^{(n+1)}}{\Delta z} = h\,((T_3)_{ijnz+1}^{(n+1)} - (T_4)_{ij0}^{(n+1)}), \end{cases} \quad z = 2H + H_1, \tag{23d}$$

and on the other boundaries,

$$(T_m)_{ijk}^{(n+1)} = T_\infty, \quad (m = 1, 2, 3, 4). \tag{23e}$$

$\{(T_m)_{ijk}^{(n+1)}\}(m = 1, 2, 3, 4)$ are computed by equation (17) line by line in the $z$-direction. As such, we express these equations as four tridiagonal linear systems:

$$-b_k^1 (T_1)_{ijk-1}^{(n+1)} + a_k^1 (T_1)_{ijk}^{(n+1)} - c_k^1 (T_1)_{ijk+1}^{(n+1)} = d_{ijk}^1, \quad k = 1, \cdots, N_z, \tag{24a}$$

$$-b_k^2 (T_2)_{ijk-1}^{(n+1)} + a_k^2 (T_2)_{ijk}^{(n+1)} - c_k^2 (T_2)_{ijk+1}^{(n+1)} = d_{ijk}^2, \quad k = 1, \cdots, N_z, \tag{24b}$$

$$-b_k^3 (T_3)_{ijk-1}^{(n+1)} + a_k^3 (T_3)_{ijk}^{(n+1)} - c_k^3 (T_3)_{ijk+1}^{(n+1)} = d_{ijk}^3, \quad k = 1, \cdots, N_z, \tag{24c}$$

$$-b_k^4 (T_4)_{ijk-1}^{(n+1)} + a_k^4 (T_4)_{ijk}^{(n+1)} - c_k^4 (T_4)_{ijk+1}^{(n+1)} = d_{ijk}^4, \quad k = 1, \cdots, N_z, \tag{24d}$$

where $i = 1, \ldots, N_x$ and $j = 1, \ldots, N_y$. Since $\{(T_m)_{ijk}^{(n+1)}\}(m = 1,2,3,4)$ is unknown at the interface between layers, the above four tridiagonal linear systems cannot be solved. To overcome this difficulty, we apply the parallel "divide and conquer" procedure for tridiagonal linear system. As such, a domain decomposition algorithm for thermal analysis in the X-ray irradiation process can be described as follows:

*Step 1.* calculate the coefficients as listed in step 1 of the parallel "divide and conquer" procedure

*Step 2.* substitute the following six equations

$$(T_1)_{ijNz}^{(n+1)} = \beta_{Nz}^{(1)} (T_1)_{ijNz+1}^{(n+1)} + v_{Nz}^{(1)}, \quad (T_2)_{ijNz}^{(n+1)} = \beta_{Nz}^{(2)} (T_2)_{ijNz+1}^{(n+1)} + v_{Nz}^{(2)} + \lambda_{Nz}^{(2)} (T_2)_{ijo}^{(n+1)},$$

$$(T_2)_{ij1}^{(n+1)} = \tilde{\beta}_1^{(2)} (T_2)_{ijo}^{(n+1} + \tilde{v}_1^{(2)} + \tilde{\lambda}_1^{(2)} (T_2)_{ijNz+1}^{(n+1)},$$

$$(T_3)_{ijNz}^{(n+1)} = \beta_{Nz}^{(3)} (T_3)_{ijNz+1}^{(n+1)} + v_{Nz}^{(3)} + \lambda_{Nz}^{(3)} (T_3)_{ijo}^{(n+1)},$$

$$(T_3)_{ij1}^{(n+1)} = \tilde{\beta}_1^{(3)}(T_3)_{ijo}^{(n+1)} + \tilde{v}_1^{(3)} + \tilde{\lambda}_1^{(3)}(T_3)_{ijNz+1}^{(n+1)}$$

$$\text{and } (T_4)_{ij1}^{(n+1)} = \tilde{\beta}_1^{(4)}(T_4)_{ijo}^{(n+1)} + \tilde{v}_1^{(4)}$$

into discrete boundary Equations (23b)-(23d) to obtain

$$(T_1)_{ijNz+1}^{(n+1)},\ (T_2)_{ijo}^{(n+1)},\ (T_2)_{ijNz+1}^{(n+1)},\ (T_3)_{ijo}^{(n+1)},\ (T_3)_{ijNz+1}^{(n+1)} \text{ and } (T_4)_{ijo}^{(n+1)}.$$

Step 3. solve for the rest of the unknowns in

$$\left\{(T_m)_{ijk}^{(n+1)}\right\}(m = 1, 2, 3, 4)$$

by step 3 of the procedure.

The above iterations are continued until a criterion for convergence is satisfied.

## 6. Numerical examples

To demonstrate the applicability of the numerical procedure we investigate the maximum temperature rise within the resist. PMMA and silicon were used as the resist and substrate, respectively. Properties of mask, gap, PMMA and silicon used in the analysis are listed in Table I. We followed the assumption in Ameel (1994) that the resist and the substrate have a linear absorption coefficient $\mu$ and are uniformly exposed with an irradiance $W_O$. A commonly used model for heat absorption in resist and substrate was chosen to be the exponential expression: (Ameel, 1994)

$$g(x, y, z) = \begin{cases} W_o \mu e^{-\mu z}, & 0 \le x \le 1 \text{ mm},\ 0 \le y \le 5\ mm, \\ 0\ , & 1 \text{ mm} < x \le 5\ mm,\ 0 \le y \le 5\ mm, \end{cases} \quad (25)$$

where the coefficients $W_O$ and $\mu$ were 3.4 W/cm$^2$ and $\frac{1}{106} \times 10^4$/cm, respectively (Ameel, 1994). Expression (25) shows that heat absorbed from the synchrotron X-ray irradiating the surface decreases exponentially with depth. For convenience, we take the exposed area to be rectangular and on the left side of the resist (Figure 1). However, it should be noted that in general the exposed area can vary in shape and position by scanning the beam on the surface of the resist. Hence, for applications in general, it is necessary to consider a three-dimensional model.

**Table I.** Thermophysical properties

| Property | PMMA | Silicon | Mask | Gap |
|---|---|---|---|---|
| $k$(W/cm/K) | $1.98 \times 10^{-3}$ | 1.50 | 2.01 | 0.152 |

Two examples are illustrated as follows. The first example is to compare the present method with our previous method for obtaining the steady state temperature by solving the unsteady state differential equations (see Dai *et al.*, 1997). In this example, we only considered the resist and substrate case and assumed that the thickness of the resist and substrate was 100μm, respectively. A convection coefficient $h_c = 0.006 W/cm^2/K$ was chosen for the top of the resist. We chose a mesh of $50 \times 50 \times 50$ for each layer. The convergent solution was obtained when $Max|T^{(n+1)} - T^{(n)}| \leq 0.5 \times 10^{-3}$ was satisfied.

Based on the above parameters, the solution obtained gave a maximum temperature rise within the resist of 5.735 K. This result is very close to 5.721 K obtained by our previous method (Dai *et al.*, 1997). Information on the temperature profile can be obtained from the three-dimensional numerical method. Figure 2 shows the temperature profile along the vertical axis at $x$ = 0.7mm and $y$ = 2.5mm, where the maximum temperature rise occurs. This profile also agreed well with that obtained by our previous method. Further results on the temperature field were given by the plot of isotherms in Figures 3 and 4. Results are also similar to those obtained by our previous method. Figure 5 gives the temperature profiles along the vertical line in the resist (where the maximum temperature rise occurs) for various grids when $\alpha = 0.95$. These results show that the present method is accurate and the solution is not significantly affected by grid size.

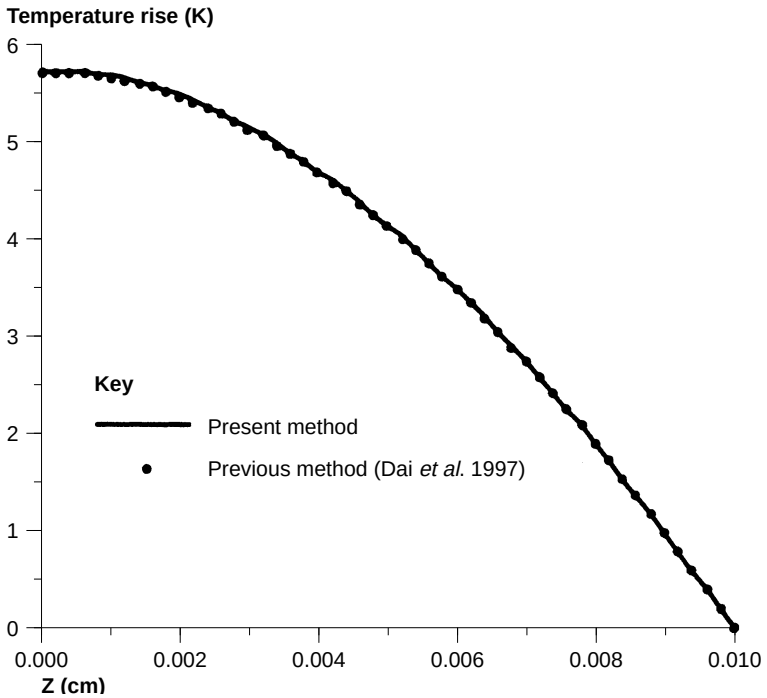


**Figure 2.**
Temperature profile at x = 0.7mm and y = 2.5mm in the resist

A convergence history with various values of the relaxation parameter, $\alpha$, is listed in Table II. Results show that the convergence is fast if $\alpha$ is close to 1. This coincides with that expected from the previous theoretical analysis. Furthermore, it took only about 4 minutes CPU in a SUN workstation to obtain the convergent solution when = 0.95, while our previous method (Dai *et al.*, 1997) took about 30 minutes CPU in the same workstation. This shows that the present method is fast in converging to the steady state solution.

The second example is to apply the present method to a commercially applicable X-ray irradiation process, where the target consists of a mask, a resist

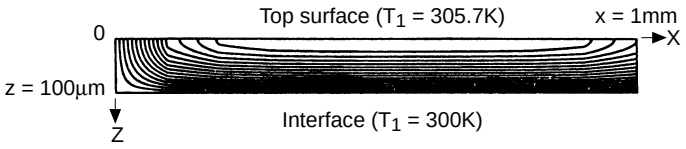


**Figure 3.**
Contour of the temperature distribution for the exposed portion of the resist at the cross section of y = 2.5mm

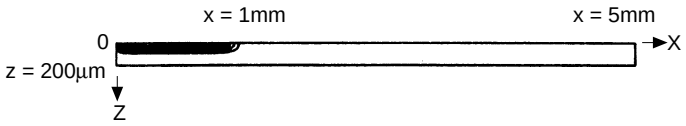


**Figure 4.**
Contour of the temperature distribution at the cross section of y = 2.5mm

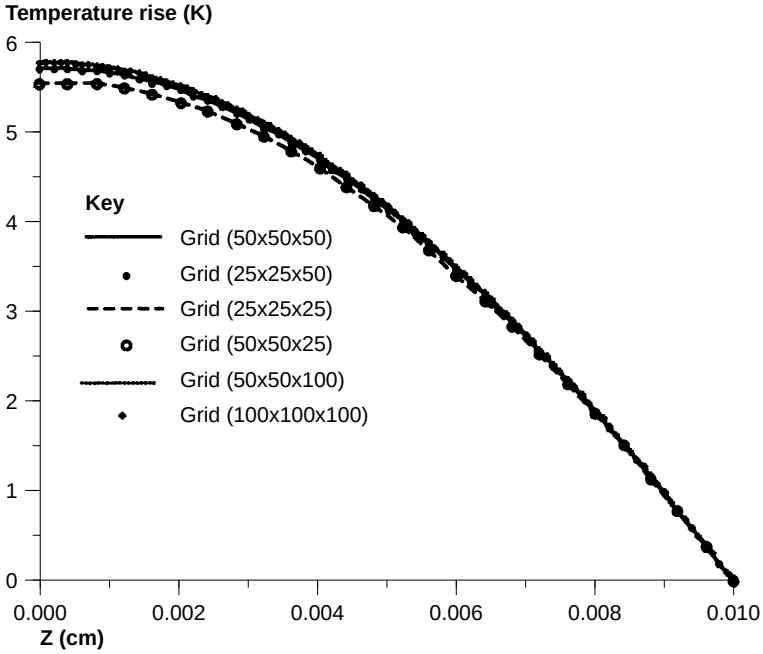


**Figure 5.**
Temperature profiles for various grids along the vertical line in the resist (where the maximum temperature rise occurs)

and a substrate (with a gap between mask and resist), as shown in Figure 1. We assumed that heat is transferred through the mask and the gap, $g(x,y,z) = 0$ for the mask and the gap. Furthermore, we chose a convection coefficient $h_c$ = 0.006W/cm$^2$/K for the top of the mask. We chose a mesh of $50 \times 50 \times 50$ for each layer. The convergent solution was obtained when $Max|T^{(n+1)} - T^{(n)}| \leq 10^{-3}$ was satisfied.

Based on the above parameters, the solution obtained gave a maximum temperature rise within the resist of 5.51K. Information on the temperature profile can be obtained from the three-dimensional numerical method. Figure 6 shows the temperature profile along the vertical axis at $x$ = 0.7mm and $y$ = 2.5mm. Further results on the temperature field are given by the plot of isotherms in Figures 7 and 8.

A convergence history with various values of the relaxation parameter, $\alpha$, is listed in Table III. Results show that the convergence is fast if $\alpha$ is close to 1. Again, this coincides with that expected from the previous theory. Furthermore, it took only about ten minutes CPU in a SUN workstation to obtain the convergent solution when $\alpha$ = 0.95.

| $\alpha$ | n |
|---|---|
| 0.95 | 31 |
| 0.9 | 33 |
| 0.8 | 37 |

**Table II.**
Number of iterations as a function of relaxation parameter, $\alpha$, for the first example

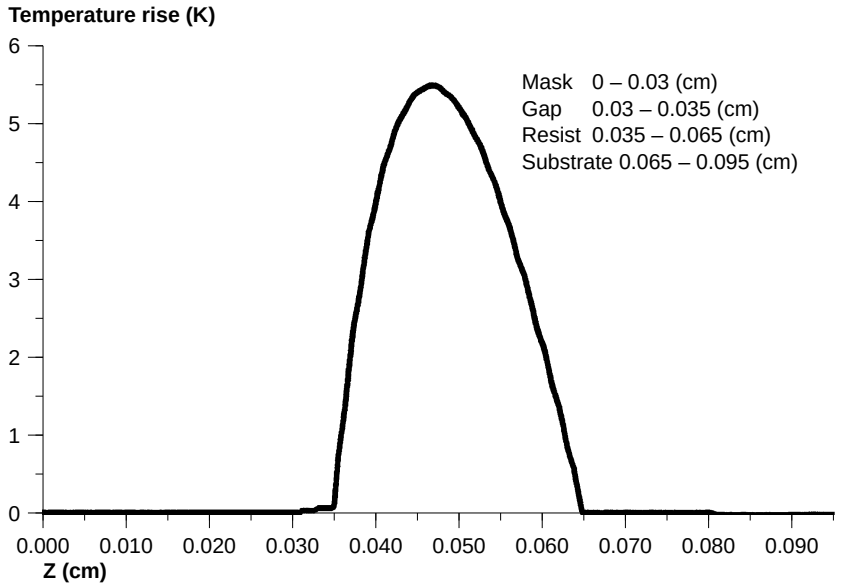


**Figure 6.**
Temperature profile along the vertical line at x = 0.7mm and y = 2.5mm

## 7. Conclusion

A three-dimensional numerical method was developed for simulating the temperature profile in an X-ray irradiation process by applying a preconditioning technique and the Richardson method for the Poisson equation in the micro-scale. The domain decomposition algorithm was then obtained based on the parallel "divide and conquer" procedure for solving tridiagonal linear systems. Numerical results show that such a method is efficient. The method can be also used for thermal analysis of thin multi-films, such as that occurring in a laser chemical vapor deposition process.

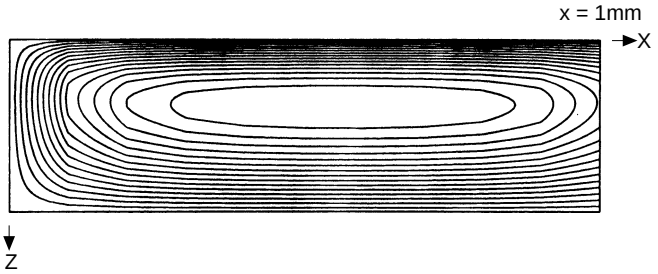


**Figure 7.**
Contour of the temperature distribution for the exposed portion of the resist at the cross section of y = 2.5mm

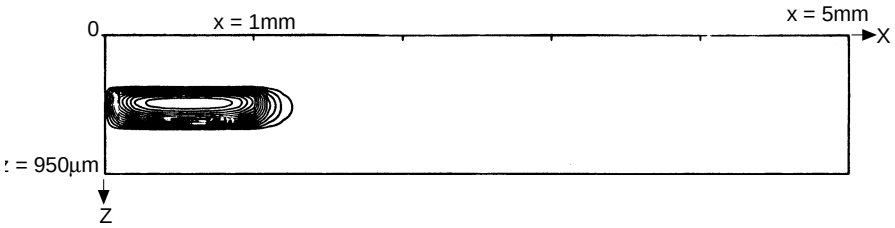


**Figure 8.**
Contour of the temperature distribution at the cross section of y = 2.5mm

**Table III.**
Number of iterations as a function of relaxation parameter, $\alpha$, for the second example

| $\alpha$ | n |
|---|---|
| 0.95 | 57 |
| 0.9 | 59 |
| 0.8 | 66 |

### References and further reading

Ameel, T.A., Warrington, R.O., Yu, D. and Dahlbacka, G. (1994), "Thermal analysis of X-ray irradiated thick resists to determine induced structural deformations", *Heat Transfer,* Vol. 4, pp. 313-18.

Canuto, C., Hussaini, M.Y., Quarteroni, A. and Zang, T.A. (1988), *Spectral Methods in Fluid Dynamics,* Springer-Verlag, New York, NY.

Cole, K.D. and McGahan, W.A. (1993), "Theory of multilayers heated by laser absorption", *Journal of Heat Transfer,* Vol. 115, pp. 767-71.

Dai, W. and Nassar, R. (1997), "A generalized Douglas ADI method for solving three-dimensional parabolic differential equations on multilayers", *Int. J. Numerical Methods for Heat & Fluid Flow,* Vol. 7 No. 7, pp. 659-74.

Dai, W. and Nassar, R., "A three-dimensional numerical model for thermal analysis in X-ray irradiated photoresists with cylindrical domain", *Numerical Heat Transfer, Part A,* in press.

Dai, W., Nassar, R., Warrington, R.O. and Shen, B. (1997), "Three-dimensional numerical models for thermal analysis in X-ray irradiated photoresists", *Numerical Heat Transfer, Part A,* Vol. 31, pp. 585-95.

Deville, M.O., Mund, E.H. and Van Kemenade, V. (1994), "Preconditioned Chebyshev collocation methods and triangular finite elements", *Comput. Methods Appl. Mech. Engrg.,* Vol. 116, pp. 193-200.

Incropera, F.P. and Dewitt, D.P. (1985), *Fundamentals of Heat and Mass Transfer,* 2nd ed., John Wiley & Sons, New York, NY.

Kant, R. (1988), "Laser-induced heating of a multilayered medium resting on a half-space: part I – stationary source", *Journal of Applied Mechanics,* Vol. 55, pp. 93-7.

Li, R. and Hong, G. (1979), *Numerical Solutions for Partial Differential Equations,* People's Educational Publisher, Peking (Chinese).

Madison, M.R. and McDaniel, T.W. (1989), "Temperature distributions produced in an N-layer by static or scanning laser or electron beam with application to magneto-optical media", *J. Appl. Phys.,* Vol. 66, pp. 5738-48.

Ottega, J.M. (1988), *Introduction to Parallel and Vector Solution of Linear Systems,* Plenum Press, New York, NY.

Ozisik, M.N. (1980), *Heat Conduction,* John Wiley & Sons, New York, NY.